JOURNAL OF MATERIALS SCIENCE 27 (1992) 4381–4388

# Development of temperature–heating rate diagrams for the pyrolytic removal of binder used for powder injection moulding

I. E. PINWILL, M. J. EDIRISINGHE*, M. J. BEVIS
*Department of Materials Technology, Brunel University, Uxbridge, Middlesex, UB8 3PH, UK*

A polypropylene-based binder system was used to injection mould test bars containing 65 vol % aluminium powder. Specimens, 3 and 6 mm thick, made from these bars were used for pyrolytic binder removal experiments in static air and nitrogen. The development of a carefully defined experimental procedure for the determination of the heating rate at which binder removal can be carried out at a given temperature without the creation of macro defects is fully described. The use of isothermal heat treatments during pyrolysis are also considered and results are presented as temperature–heating rate diagrams for each atmosphere and thickness investigated. These diagrams show a lower and an upper boundary. Defect formation occurs if the temperature–heating rate relationship lies between the boundaries. Near optimum binder removal schedules deduced from each diagram have been experimentally verified.

## 1. Introduction

Injection moulding is an attractive method for the automated mass production of geometrically complicated, dimensionally accurate engineering components with both metal and ceramic powders [1, 2]. The powder is finely dispersed in a binder system in order to make flow into a shape-forming tool possible. However, the binder is subsequently removed, mainly by pyrolysis, before sintering the components in order to achieve a high density. The binder removal stage is less well developed and tends to cause high scrap rates [3, 4], especially in thick sections of submicrometre size powder assemblies [5].

Systematic development of the pyrolytic binder removal process has started only recently [6–8]. Thus there is no general basis behind the several non-linear binder removal temperature–time schedules quoted in the literature, except that the heating rate up to the softening point of the powder–binder formulation is rapid in comparison with that used during the actual pyrolytic degradation of the binder system, and reasons for this have been discussed [9]. It is necessary to modify temperature–time pyrolysis schedules to suit the binder system used [10, 11] and the powder which could in some instances catalyse thermal decomposition [12, 13].

A binder system contains several components [14]. The major binder determines the overall properties of the binder system but low molecular weight minor binders are usually added to enhance the fluidity of the suspension and aid binder removal. In addition, the formulation contains a small amount of processing aid, in most instances stearic acid [15], which improves the wettability between the powder and the binders. Polypropylene has been identified as a successful major binder [16–18] and an isotactic polypropylene, microcrystalline wax, stearic acid binder system in the weight ratio 6:2:1 gives excellent flow properties [19] for the injection moulding of concentrated suspensions [20].

In the present work, using aluminium powder as the filler and the above-mentioned polypropylene–wax–stearic acid composition as the binder system, a carefully controlled experimental procedure, necessary for the construction of diagrams which indicate the correct temperature–heating rate relationship for macro-defect-free binder removal from injection-moulded bars, is described. The effect of the atmosphere used for binder removal and the thickness of the mouldings on the temperature–heating rate relationship were also investigated. The near optimum heating rate–temperature schedule for macro-defect-free binder removal under each set of conditions was deduced from the relevant diagram and experimentally verified.

## 2. Experimental details

### 2.1. Materials

Commercial purity aluminium powder (99.6 wt % Al, impurities Fe, Si, Zn, specific surface area 0.33 $m^2 g^{-1}$) was used as the filler. The particle-size distribution and shape of this powder are shown in Fig. 1a and b. Details of the polypropylene-based binder system used are given in Table I.

*Author to whom all correspondence should be addressed.

0022–2461 

TABLE I Details of constituents in the binder system

| Name | Grade | Density ($kg\ m^{-3}$) | Molecular weight ($\bar{M}_n$) | Supplier |
|---|---|---|---|---|
| Isotactic polypropylene | GY545M | 905 | 31850 | ICI Ltd, Welwyn Garden City, UK |
| Microcrystalline wax | 1865Q | 910 | 300 | Astor Chemicals Ltd, West Drayton, UK |
| Stearic acid | 302694Q | 941 | – | BDH Chemicals Ltd, Poole, UK |

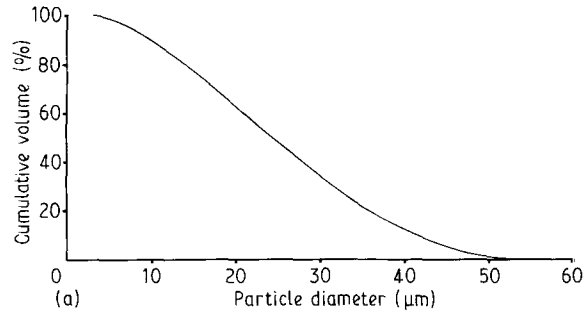


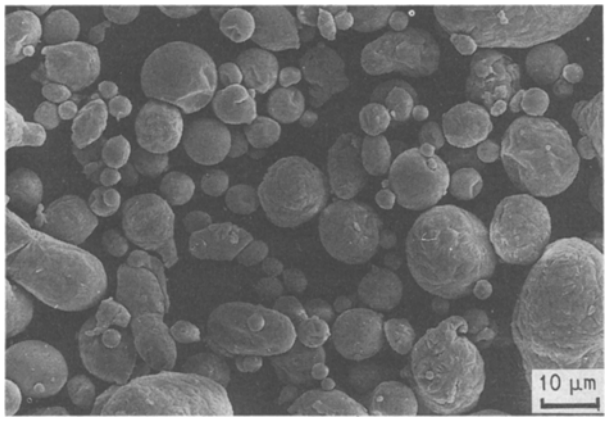


*Figure 1* (a) Particle size distribution, and (b) scanning electron micrograph of commercial purity aluminium.

## 2.2. Specimen preparation

The powder was dried at 160 °C for 30 min and then transferred to a Henschel high-speed mixer containing the stearic acid. Mixing was carried out at 2000 r.p.m. for 2 min enabling the stearic acid, which melted in the presence of hot aluminium, to coat the powder particles. The blend was cooled to room temperature before polypropylene and wax were added and mixing was continued at 2000 r.p.m. for a further 3 min. An intermeshing, co-rotating twin screw extruder was used to compound the formulation. The procedure of compounding for this organic vehicle is well documented [16] and the resulting suspension is homogeneous [21]. A formulation with nominally 65 vol % Al was prepared in this manner. The extrudate was granulated and the exact volume loading of filler was verified by ashing three samples of the formulation.

Granules of the formulation were injection moulded to produce nominally 6 mm thick test bars using a Sandretto 6GV/50 reciprocating screw machine. The test bars were X-ray radiographed in order to ensure that they were free of macro-defects, such as voids and cracks, before binder removal. Specimens, 3 and 6 mm thick, for binder removal studies were made using these test bars as illustrated in Fig. 2.

## 2.3. Equipment

A model HT-D Stanton automatic thermobalance was used in conjunction with a model 2054 Gulton West temperature controller. The balance allowed carefully controlled binder removal experiments to be carried out with the weight loss measurements being useful during specimen removal as discussed later (Section 2.4.2). The temperature controller allowed the use of accurate heating rates down to $1\ °C\ h^{-1}$ with programmable facilities giving up to 32 separate heating ramp/dwell cycles per experiment. A thermocouple located close to the specimen was used to monitor the temperature which was corrected to determine the actual specimen temperature.

Experiments were carried out in both static air and flowing oxygen-free nitrogen. The nitrogen was dried by passing through $CaCl_2$ and activated alumina before entering the specimen chamber. The flow rate used was $2\ l\ min^{-1}$, more than sufficient to prevent oxidation of copper powder during the 20–450 °C temperature range used for binder removal. Specimens 3 and 6 mm thick were positioned in an alumina crucible and on a stainless steel gauze, respectively, during binder removal. However, specimens were largely unsupported so that the possibility of slumping was not prevented and the escape of volatile degradation products was not hindered.

## 2.4. Development of diagrams

### *2.4.1. Procedure*

Heating rates used were 128, 64, 32, 16, 8, 4, 2 and $1\ °C\ h^{-1}$.

The lower boundaries of the temperature–heating rate diagrams were determined as described below.

A specimen was placed in the furnace of the thermobalance and heated at $128\ °C\ h^{-1}$ to a temperature which was in the ranges 20–300 and 20–450 °C for static air and flowing nitrogen, respectively. The specimen was removed on reaching the final temperature according to the procedure described later (Section 2.4.2). It was inspected visually and, if necessary, by low-power optical microscopy, to determine whether

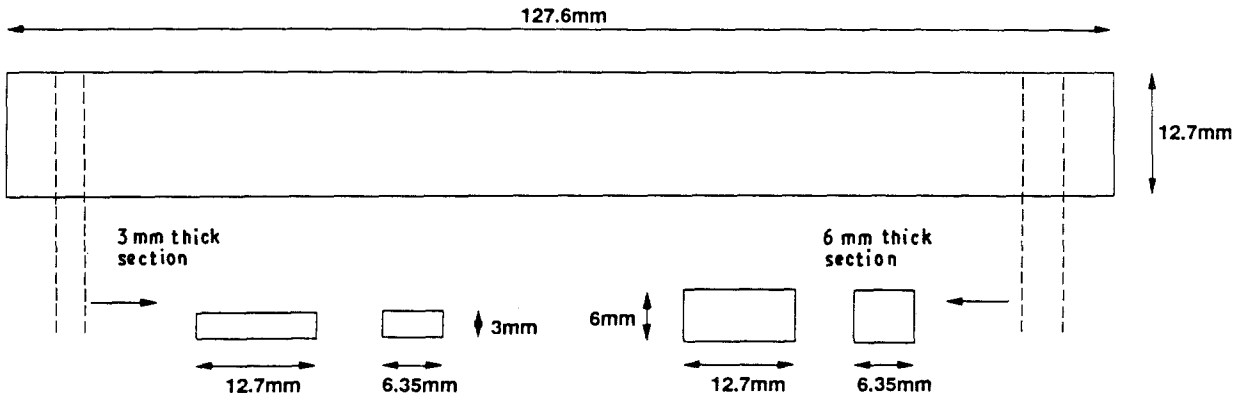


*Figure 2* Dimensions of injection-moulded test bars and specimens used for binder removal experiments.

macro-defects were present. The experiment was carried out at a temperature 20 °C lower if defects were present. Otherwise, it was repeated at a temperature 20 °C higher. Depending on the initial outcome, this procedure was repeated until defects appeared or were completely removed.

When a defect was eliminated or generated by the 20 °C change, the temperature at which it just forms was determined by investigating the temperature interval more closely. This was done by repeating the experiment several times, reducing the 20 °C temperature interval as necessary. Once the temperature at which the defect just forms was determined it could be plotted on a graph of temperature versus heating rate. The whole process was then repeated for the other heating rates, in decreasing order, until one of two things happened:

(i) a heating rate was reached at which defects were not formed at any temperature;

(ii) all heating rates produce defects.

It was necessary to introduce an isothermal hold if defects formed when heating to a temperature even at 1 °C $h^{-1}$. The minimum duration of this hold was determined in a similar manner to that used for estimating the temperature at which defects just form for a given heating rate.

The upper boundary of each diagram was determined in an identical manner. However, if the time required to remove the binder up to the lower boundary temperature was excessive, this being the case in flowing nitrogen, the experimental procedure was speeded up by using a specimen in which binder removal had taken place to near the lower boundary temperature. The production of a large batch of specimens which satisfied this condition, was carried out in a muffle furnace, in flowing nitrogen, using a heating rate of 1 °C $h^{-1}$. This was followed by "quenching" to room temperature according to the specimen removal procedure described in Section 2.4.2. When these specimens were used in binder removal experiments they were rapidly reheated to the temperature at which binder removal was terminated without introducing defects. Trial and error experiments showed that, to satisfy this, reheating should be done at 64 °C $h^{-1}$ to 4 °C below the required temperature followed by 4 °C $h^{-1}$ to the final temperature. Obviously, there was loss of binder associated with this reheating process and it could be expected to affect the upper boundary temperature at which the heating rate could be increased during binder removal. Therefore, when this method was employed, the upper boundaries of the affected diagrams are represented by dotted lines. However, upper boundaries of this type were again verified by carrying out experiments where the full pyrolysis was done according to the temperature ramp indicated by the relevant diagram.

### 2.4.2. Specimen removal

In the case of experiments in static air, the furnace of the thermobalance was turned off and slowly lifted when the test temperature was reached. The specimen was allowed to sit just within the neck of the furnace tube for 2 min before being fully exposed to ambient conditions. This minimized thermal shock and prevented cracking, especially during cooling from high test temperatures.

A slightly modified procedure was followed in experiments done in flowing nitrogen. The furnace was turned off when the required temperature was reached and the flow rate of the nitrogen was increased as much as possible without disturbing specimen weight loss measurements. The furnace was then raised so that the specimen was moved to a much cooler zone. Care was taken to prevent oxygen diffusion to the cooling specimen as it would cause rapid oxidative degradation of the binder system creating defects. Any diffusion of oxygen during cooling was easily detected as this caused a sharp increase in weight loss. Trial and error experiments revealed that to prevent oxygen diffusion the specimen should sit at least 50 mm from the end of the furnace tube. The specimen was allowed to sit in this position for at least 15 min before exposure to ambient conditions in order to examine for defects.

## 2.5. Verification of diagrams

The near optimum heating rate–temperature binder removal schedule deduced from each diagram was verified by performing thermogravimetric experiments using the relevant sample thickness and debinding atmosphere. Weight loss versus temperature data was recorded and specimens produced were subjected to visual and low-magnification optical microscopy examination.

An as-moulded 6 mm thick bar was subjected to binder removal in static air using a muffle furnace according to the relevant near optimum binder removal schedule. The product was visually examined and further investigated using X-ray radiography.

## 3. Results and discussion

Ashing experiments revealed that the formulation contained 64.7 ( $\pm$ 0.04) vol % aluminium.

### 3.1. Binder removal in static air

In static air, oxidative degradation of the binder takes place preferentially at the surface regions of the specimen while thermal degradation occurs at the core. The temperature–heating rate diagram for the 3 mm thick specimens subjected to binder removal in static air (Fig. 3a) shows that the lower boundary is between 152 and 168 °C at heating rates of 128 and 8 °C $h^{-1}$, respectively. A heating rate of 4 °C $h^{-1}$ produced macro-defect-free specimens at all temperatures. The nose of the curve will therefore be between 4 and 8 °C $h^{-1}$ and because its position was not determined exactly it is indicated by a dotted line in Fig. 3a. The upper boundary shows that the heating rate can be initially increased to 8 °C $h^{-1}$ at 200 °C and then progressively to 128 °C $h^{-1}$ at 280 °C. The optimum binder removal schedule for these conditions can be obtained by following the contour shown in Fig. 3a (and similar diagrams for other conditions). However, in order to reduce the large number of heating ramp/dwell cycles, a near optimum binder removal schedule for this formulation and specimen thickness in static air derived from Fig. 3a is given in Table II. Thus it takes approximately 14 h to oxidatively remove the binder from this thickness of specimen without introducing defects.

The equivalent diagram for the 6 mm thick specimens (Fig. 3b) shows a similar pattern, with the lower

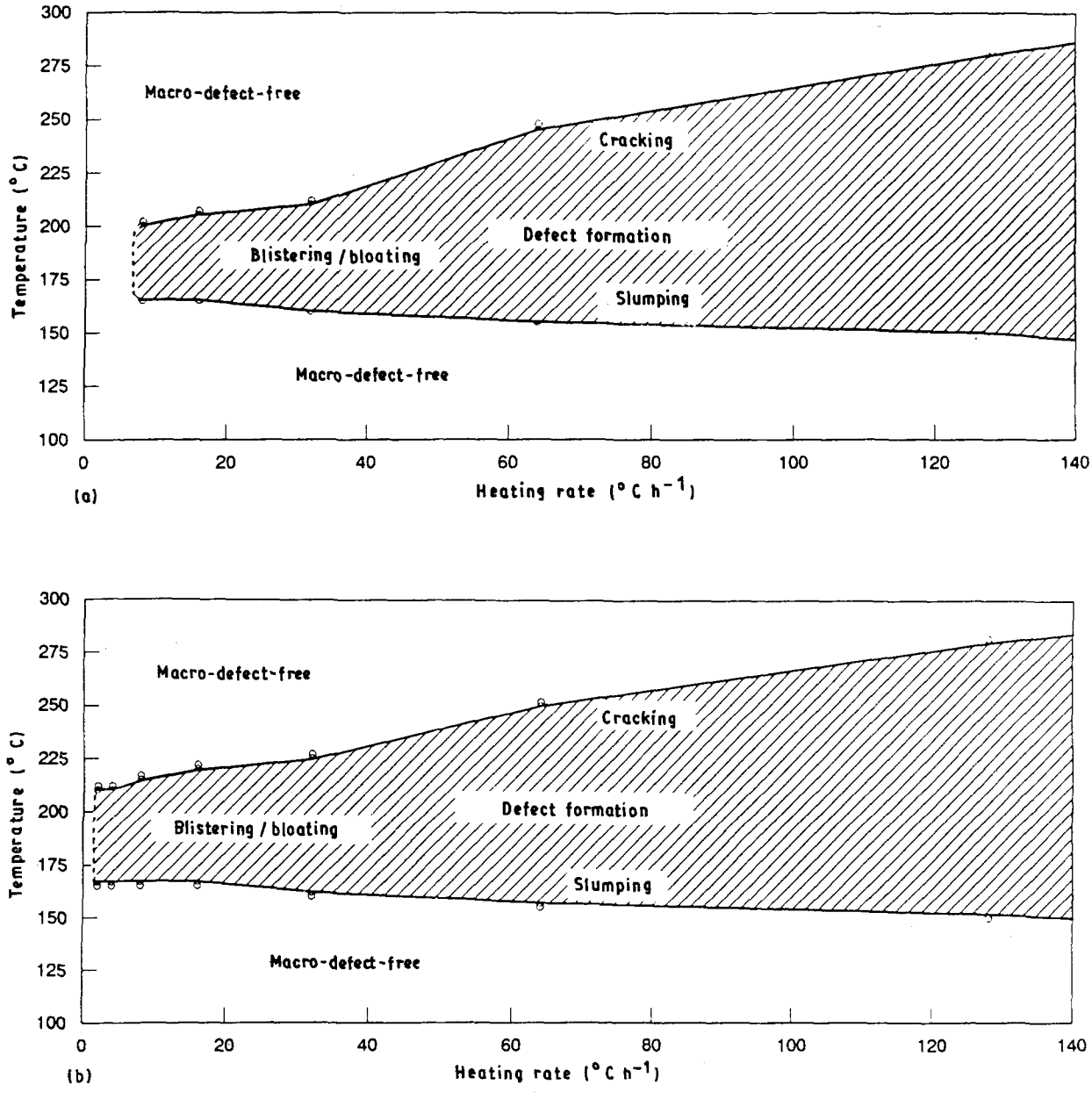


*Figure 3* Temperature–heating rate diagrams showing binder removal from (a) 3 mm and (b) 6 mm thick specimens in static air, and (c) 3 mm and (d) 6 mm thick specimens in flowing nitrogen.

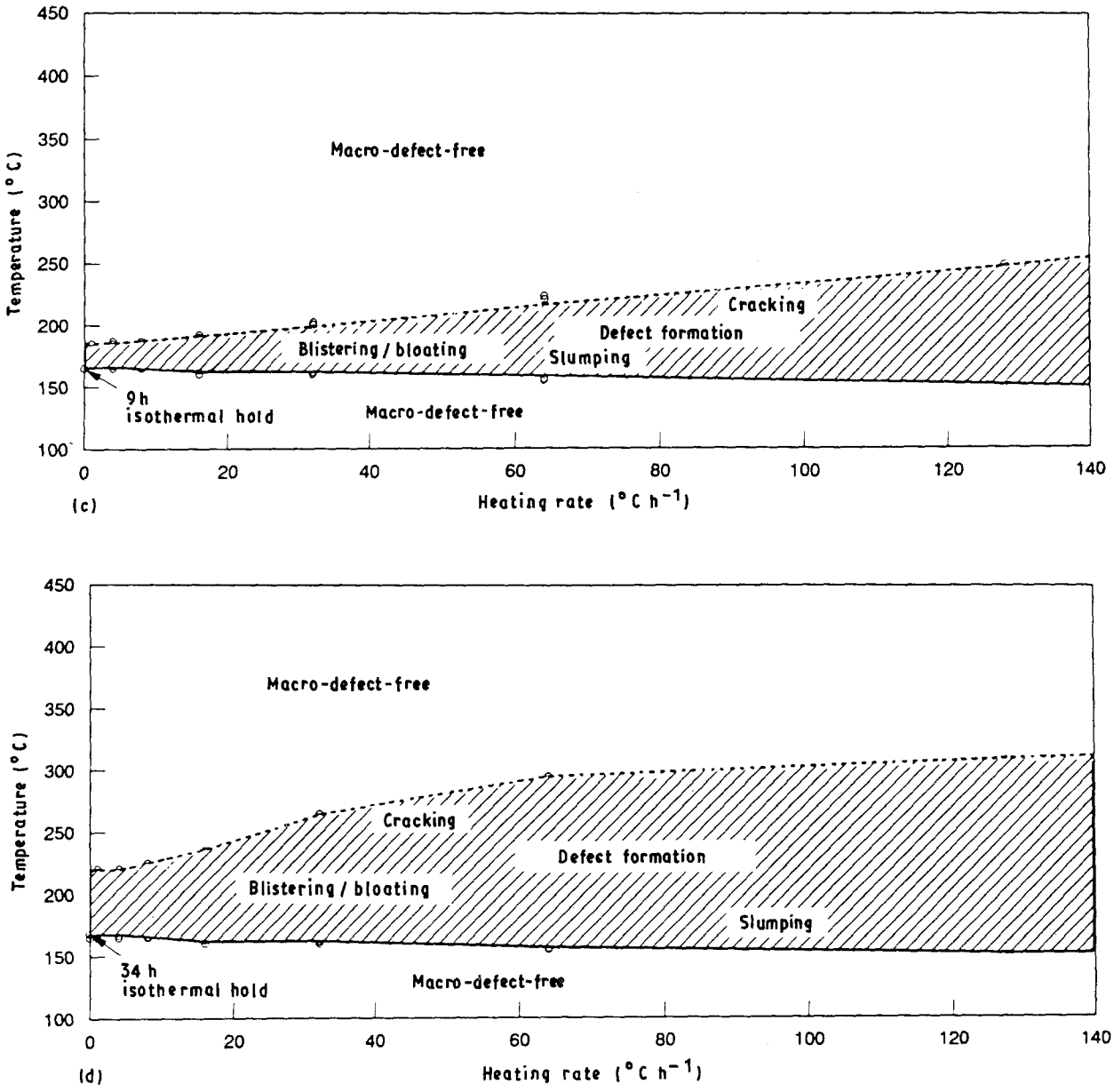


*Figure 3* Continued

boundary of defect formation occurring between 152 and 167 °C at heating rates of 128 and 2 °C $h^{-1}$, respectively. In this instance, a heating rate of 1 °C $h^{-1}$ gave no defects at any temperature. Compared to the diagram for the 3 mm thickness (Fig. 3a) the upper boundary varies to a lesser extent due to increase in the rate of heating. However, a minimum temperature of 210 °C must be reached during binder removal in order to progress to a faster heating rate than 1 °C $h^{-1}$ without forming defects. This leads to an effective enlargement in the defect formation window. The near optimum binder removal schedule for this thickness of specimen is given in Table II and is of about 49 h duration. Compared with the duration for the 3 mm section size this is an increase of 3.5 times which is purely due to doubling the thickness and is in broad agreement with the work of German [22] who states that the binder removal time is directly proportional to the square of the section thickness. It is worth noting that oxidative binder removal schedules could also be affected by the shape of the moulding [23].

Each diagram indicates the defect types encountered when incorrect temperature–heating rates relationships are used. The diagrams confirm that heating to temperatures near the softening point of the formulation (approximately 150 °C) can be done rapidly. However, if the softening point of the formulation is exceeded at a heating rate in excess of 4 °C $h^{-1}$ for the 3 mm thick specimens (decreases to 1 °C $h^{-1}$ when the thickness is doubled), then slumping occurs. Heating well past the softening point at a heating rate in excess of the predicted values caused blistering and bloating. Thus the softening point is an important temperature in binder removal practice. Faster heating rates can be used during the later stages of pyrolysis when porosity has been created due to loss of some binder, making outward diffusion of decomposition products easier. Cracking occurs if a fast heating rate is engaged too soon. Here surface and internal cracks form if the generation of volatile components within the moulding is in excess of the amount removed by outward diffusion and evaporation at the surface at a given

TABLE II Near optimum binder remover schedules for 3 and 6 mm thick mouldings in static air and flowing nitrogen

| Atmosphere | Thickness (mm) | Temperature range (°C) | Heating rate (°C h$^{-1}$) |
|---|---|---|---|
| Air | 3 | 20–150 | 128 |
| | | 150–156 | 64 |
| | | 156–162 | 32 |
| | | 162–168 | 16 |
| | | 168–200 | 4 |
| | | 200–205 | 8 |
| | | 205–210 | 16 |
| | | 210–245 | 32 |
| | | 245–280 | 64 |
| | | 280–500 | 128 |
| | 6 | 20–150 | 128 |
| | | 150–156 | 64 |
| | | 156–162 | 32 |
| | | 162–168 | 16 |
| | | 168–210 | 1 |
| | | 210–215 | 4 |
| | | 215–220 | 8 |
| | | 220–225 | 16 |
| | | 225–250 | 32 |
| | | 250–280 | 64 |
| | | 280–500 | 128 |
| Nitrogen | 3 | 20–150 | 128 |
| | | 150–155 | 64 |
| | | 155–160 | 32 |
| | | 160–165 | 8 |
| | | 165 | hold for 9 h |
| | | 165–175 | 1 |
| | | 175–180 | 4 |
| | | 180–190 | 8 |
| | | 190–200 | 16 |
| | | 200–220 | 32 |
| | | 220–245 | 64 |
| | | 245–500 | 128 |
| | 6 | 20–150 | 128 |
| | | 150–155 | 64 |
| | | 155–160 | 32 |
| | | 160–165 | 8 |
| | | 165 | hold for 34 h |
| | | 165–220 | 1 |
| | | 220–225 | 4 |
| | | 225–235 | 8 |
| | | 235–265 | 16 |
| | | 265–295 | 32 |
| | | 295–310 | 64 |
| | | 310–500 | 128 |

temperature. During the later stages of binder removal the moulding is in a brittle pseudo-solid state and this makes it more susceptible to cracking rather than blistering or bloating.

## 3.2. Binder removal in flowing nitrogen

In this instance, thermal degradation of the binder system occurs throughout the specimen. The lower boundary of the temperature versus heating rate diagram for the 3 mm thick specimen (Fig. 3c) varies from 152–167 °C at heating rates of 128 and 1 °C h$^{-1}$, respectively. The fact that the lowest heating rate of 1 °C h$^{-1}$ used in the experiments still caused defects meant that an isothermal hold needed to be introduced into the binder removal schedule. In this instance, 9 h was the required hold time before a heating rate of 1 °C h$^{-1}$ could be reintroduced without slumping taking place. The upper boundary shows that a heating rate of 1 °C h$^{-1}$ needs to be maintained to 185 °C before it can be increased progressively. The near optimum debinding schedule deduced from this diagram is given in Table II. Time for complete binder removal was about 28 h.

The effect of doubling the section thickness to 6 mm is shown in Fig. 3d. Here there is negligible change in the lower boundary except for the fact that there is a considerable increase necessary in the isothermal hold time; 34 h were required before a heating rate of 1 °C h$^{-1}$ could be reintroduced. The upper boundary shows that after the isothermal hold the temperature can be increased at 1 °C h$^{-1}$ to 220 °C which is 35 °C higher compared to the smaller thickness. The window of defect formation has also considerably widened. These features indicate a substantial increase in debinding time. The near optimum binder removal schedule derived from the diagram is given in Table II. According to this, the time required for the binder extraction is about 100 h which again is an increase of 3.6 times compared to the 3 mm section size and obeying the rule suggested by German [22], mentioned earlier (Section 3.1).

Major defect types encountered were similar to those of the static air situation with the softening point of the formulation having a major influence on the position of the lower boundary. Once again, for reasons similar to those that were mentioned for the static air situation, slow heating rates used to exceed the softening point can only be increased during the later stages of binder removal. The binder removal times are considerably larger in comparison with those for the identical oxidative case mainly because oxidative degradation takes place over a lower temperature range as shown in the thermograms below. A full discussion of the reasons responsible for this difference is beyond the scope of this article and will be addressed in a future publication. It is interesting to note that for both thicknesses investigated the binder removal time was approximately double in the case of thermal degradation when compared to oxidative degradation.

## 3.3. Thermograms

There is no substantial difference in the weight loss versus temperature graphs for the two section thicknesses subjected to binder removal in static air (Fig. 4a) except for the fact that there is an increase in the final temperature required for total binder removal in the thicker moulding. This is expected as the core region of the specimen in which thermal degradation of the major binder, polypropylene, takes place is greater with increasing section size. The appearance of a shoulder at about 30 wt % binder removed with an almost linear rate of weight loss beyond this is clearly seen for both section sizes. Up to this "shoulder" evaporation of the low molecular weight species, principally the wax and stearic acid, occurs. The sharp change in rate beyond this, with approximately the

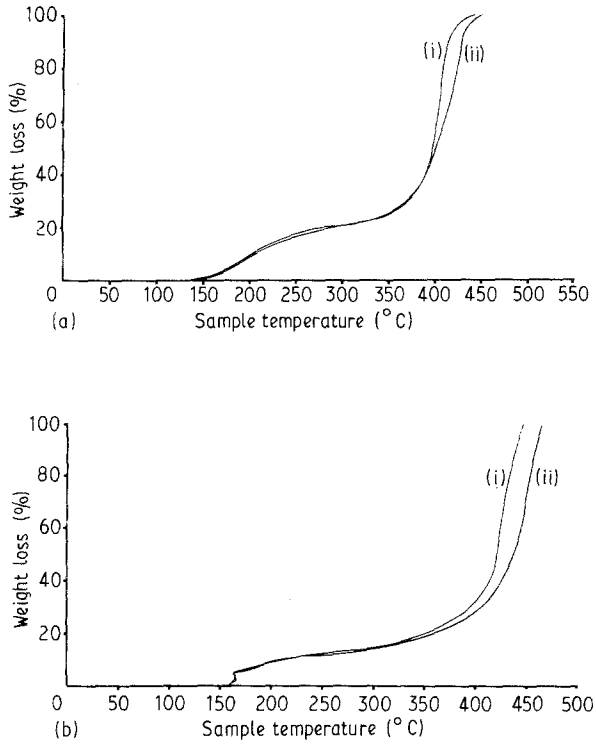


*Figure 4* Thermogravimetric traces representing binder removal in (a) static air and (b) flowing nitrogen, according to near optimum temperature–heating rate schedules given in Table II, for (i) 3 mm and (ii) 6 mm section thicknesses.

final 70 wt % binder being removed over a very narrow temperature range of about 50 °C, is due to the decomposition of polypropylene and clearly indicates that binder extraction with the rate of weight loss controlling the temperature is virtually impossible in these section thicknesses of mouldings.

The weight loss versus temperature graphs representing binder removal in nitrogen (Fig. 4b) also show considerable similarities. Again, the only appreciable difference is the increase in final temperature required for total binder removal in the thicker moulding because thermal degradation takes place over a large cross-section. As in the case of binder removal in static air, the appearance of a "shoulder", up to which the wax and stearic acid evaporates, again occurs at about 30 wt % binder extracted and is followed by the sharp weight loss over a narrow temperature range caused by the thermal decomposition of polypropylene. The temperature required for a fixed amount of binder removed is higher compared to that in static air and as observed earlier is the major reason for the increase in debinding time.

### 3.4. Verification

Visual and low-magnification optical microscopy did not reveal any defects in the specimens subjected to pyrolysis using the near optimum binder removal schedules. The 6 mm thick bar subject to pyrolysis in static air according to the near optimum binder removal schedule (Table II) showed no defects when visually examined (Fig. 5a) and subsequent X-ray radiography (Fig. 5b) too did not reveal any internal voids or cracks.

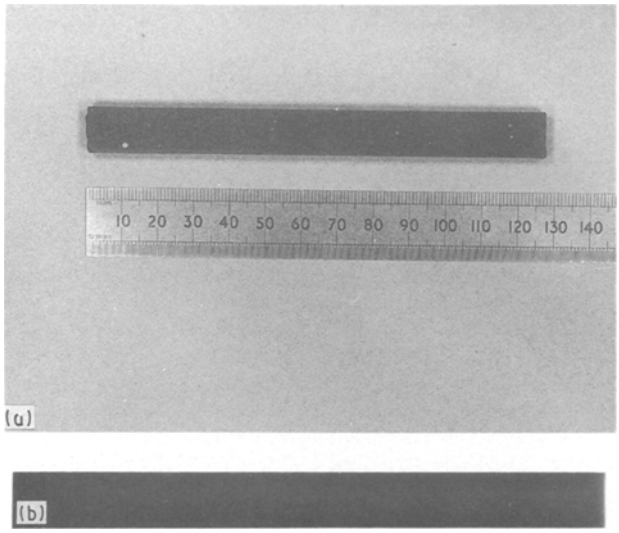


*Figure 5* 6 mm thick injection-moulded test bar subjected to binder removal in static air according to the near optimum temperature–heating rate schedule given in Table II. (a) Visual appearance, (b) X-ray radiograph.

## 4. Conclusions

Although heating rate versus temperature diagrams produced in this investigation are strictly applicable to only the aluminium–polypropylene composition investigated, it develops a procedure, which can be experimentally verified, for establishing such diagrams according to the needs of each manufacturer. In this type of process where successful binder removal depends on several factors this approach may be the only viable solution.

Doubling the section thickness almost quadruples the binder removal time which is also double in flowing nitrogen compared with static air for both thicknesses investigated. These facts make pyrolytic binder removal from large cross-section mouldings in nitrogen very time-consuming and therefore commercially unattractive.

The defects formed clearly illustrate the importance of the softening point of the formulation. When this temperature is reached, heating rates employed must be considerably reduced. However, faster heating rates can be used later on during pyrolysis.

## Acknowledgements

The authors thank SERC (UK) for funding the powder injection moulding research at Brunel. The technical help of H. Andrews is gratefully acknowledged. K. Armstrong is thanked for typing this manuscript.

## References

1. B. C. MUTSUDDY, *J. Ind. Res. Devel.* **25** (1983) 76.
2. P. K. JOHNSON, *Int. J. Powder Metall.* **15** (1979) 323.
3. J. G. ZHANG, M. J. EDIRISINGHE and J. R. G. EVANS, *Ind. Ceram.* **9** (1989) 72.
4. R. CARLSSON, *Mater. Design* **10** (1989) 10.
5. J. R. G. EVANS and M. J. EDIRISINGHE, *J. Mater. Sci.*, **26** (1991) 2081.
6. R. M. GERMAN, *Int. J. Powder Metall.* **23** (1987) 237.

7. P. D. CALVERT and M. J. CIMA, *J. Amer. Ceram. Soc.* **73** (1990) 575.
8. J. R. G. EVANS, M. J. EDIRISINGHE, J. K. WRIGHT and J. CRANK, *Proc. R. Soc. A* **432** (1991) 321.
9. J. G. ZHANG, M. J. EDIRISINGHE and J. R. G. EVANS, *Mater. Lett.* **7** (1988) 15.
10. J. WOODTHORPE, M. J. EDIRISINGHE and J. R. G. EVANS, *J. Mater. Sci.* **24** (1989) 1038.
11. J. K. WRIGHT, J. R. G. EVANS and M. J. EDIRISINGHE, *J. Amer. Ceram. Soc.* **72** (1989) 1822.
12. S. MASIA, P. D. CALVERT, W. E. RHINE and H. K. BOWEN, *J. Mater. Sci.* **24** (1989) 1907.
13. M. J. EDIRISINGHE, in "Proceedings of the 11th Risø International Symposium on Metallurgy and Materials Science: structural ceramics – processing, microstructure and properties", edited by J. J. Bentzen *et al.* (Risø National Research Laboratory, Denmark, 1990) pp. 257–62.
14. M. J. EDIRISINGHE and J. R. G. EVANS, *Int. J. High Tech. Ceram.* **2** (1986) 1.
15. M. J. EDIRISINGHE, *Ceram. Int.* **17** (1991) 89.
16. M. J. EDIRISINGHE and J. R. G. EVANS, *Brit. Ceram. Trans. J.* **86** (1987) 18.
17. S. KAMIYA, M. MURACHI, H. KAWAMOTO, S. KATO, S. KAWAKAMI and Y. SUZUKI, Publication No. 850523 (Society of Automotive Engineers, USA, 1985).
18. K. SAITO, T. TANAKA and T. HIBINO, UK Pat. 1426317, 25 February 1976.
19. M. J. EDIRISINGHE and J. R. G. EVANS, *J. Mater. Sci.* **22** (1987) 269.
20. *Idem, ibid.* **22** (1987) 2267.
21. *Idem, Proc. Brit. Ceram. Soc.* **38** (1986) 67.
22. R. M. GERMAN, *Int. J. Powder Metall.* **23** (1987) 237.
23. B. C. MUTSUDDY, in "Non-Oxide Technical Ceramics", edited by S. Hampshire (Elsevier, London, 1985) pp. 397–408.

*Received 12 April*
*and accepted 23 July 1991*